Journal of Atmospheric and Terrestrial Physics, Vol. 40, pp. 323–329. Pergamon Press, 1978. Printed in Northern Ireland

Structure of tangential discontinuities at the magnetopause: the nose of the magnetopause

M. Roth

Institut d'Aéronomie Spatiale de Belgique, 3 Avenue Circularie, 1180 Bruxelles, Belgium

Abstract—Observations show that the magnetopause can sometimes be represented as a tangential discontinuity in the magnetic field. In this paper, we use a theoretical model of steady-state tangential discontinuities to analyze the microscale structure of the nose of the magnetopause. The boundary layer is described in terms of a kinetic theory based on the Vlasov–Maxwell equations for the charged particles and electromagnetic fields. The general model represents the magnetosheath and magnetospheric sides as distinct regions with anisotropic displaced Maxwellian equilibrium states and allows the presence of a multi-component plasma whose ionic species have different concentrations, temperatures, anisotropies, etc. For the nose region, we assume for simplicity an isotropic Maxwellian hydrogen plasma. Transition profiles for the magnetic field, electric potential, electric field, charge separation and density are illustrated. The variations of the magnetic field direction in the discontinuity plane show a great variety of rotational structures in accordance with recent observations. The electric potential difference is seen to control the thickness of the magnetopause. The classical Ferraro boundary layer where the ion current is neglected is recovered when the ion distribution function is a Maxwellian everywhere in the transition. When there is no electric potential difference across the sheath we find again an 'electron-dominated' boundary layer where the electric current is mainly carried by the electrons. However, computations of drift and thermal velocities indicate that a two-stream instability occurs in the centre of these sheaths. The result will be a broadening of the layer by wave-particle interactions leading to an 'ion-dominated' transition.

1. INTRODUCTION

For a substantial fraction of single satellite magnetopause crossings the behaviour of the magnetic field component perpendicular to this boundary is now studied with a high level of confidence by use of minimum variance analysis directly from magnetometer data (Sonnerup, 1976). By this technique, Sonnerup and Ledley (1974) have interpreted more than fifty OGO 5 magnetopause crossings. Their analysis has revealed the presence of rotational discontinuities for two particular crossings. However, an impressive fraction of the other 48 magnetopause crossings appear to have an average normal component of magnetic field that is indistinguishable from zero. Neugebauer *et al.* (1974) analyzed several magnetopause crossings of OGO 5. For one case in the near Earth region of the geomagnetic tail, the structure agreed closely with a simple Chapman–Ferraro magnetopause with nearly complete neutralization of the charge separation electric field. Cummings and Coleman (1968) identified a number of relatively clear tangential discontinuities and reported no rotational structures during ATS 1 magnetopause crossings.

The theoretical model presented here describes the magnetopause as a tangential discontinuity; i.e. the most frequently observed case. The aim of this paper is to use such a theoretical model for the description of the nose region of the magnetopause. To describe the different regions of the magnetopause, a model must include boundary conditions which permit plasma flows in the discontinuity plane and temperature anisotropies at both sides of the sheath. Furthermore the model will be sufficiently general to take into account the minor constituents of the solar wind and the presence of energetic particles. The theory of this general tangential discontinuity will be presented elsewhere (Roth, 1976). Here it is summarized briefly in Section 2. In Section 3, we describe the boundary conditions and we discuss the distributions of plasmas and fields across the layer. It is shown that by a suitable choice of the electric potential difference between the two faces of the layer, we can recover a current layer similar to the classical description of the Ferraro magnetopause where the electrons carry most of the current (Ferraro, 1952). However, this boundary layer happens to be unstable. Some consequences of this instability for the magnetopause model are discussed in the concluding section.

2. THE THEORETICAL MODEL

The tangential discontinuity in the magnetic field is described in terms of a kinetic theory based on

Maxwell's equations and Vlasov's equation for each particle species. The plasma contains positive particles and electrons; each species is denoted by the superscript ν; $m^{(\nu)}$ and $Z^{(\nu)}e$ are the mass and the electric charge of the corresponding particle. The plane of the discontinuity is parallel to the Y–Z plane, and all the variables are assumed to depend on the X co-ordinate only. The state of the plasma has distinct characteristics on opposite sides of the transition (at $X = -\infty$ and $X = +\infty$, denoted by subscripts 1 and 2): perpendicular ($T_{\perp_1}^{(\nu)}$, $T_{\perp_2}^{(\nu)}$) and parallel ($T_{\parallel_1}^{(\nu)}$, $T_{\parallel_2}^{(\nu)}$) temperatures, densities ($N_1^{(\nu)}$, $N_2^{(\nu)}$) and bulk velocity components (V_{y_1}, V_{y_2} and V_{z_1}, V_{z_2}). The magnetic field is parallel to the Y–Z plane and has given distinct intensities (B_1, B_2) and directions (θ_1, θ_2) on the two sides. The polarization and induced electric field is along the X-axis and there is no plasma transport across the discontinuity.

This model differs from that of ALPERS (1969, 1971) and KAN (1972), who also considered multidirectional currents but assumed exactly charge neutral layers. It completes the model of LEMAIRE and BURLAGA (1976) describing diamagnetic boundary layers in the solar wind by including bulk speeds and anisotropies on the two sides of the discontinuity surface.

Evidently there is a great choice of velocity distribution functions which are solutions of Vlasov's equation. We have been guided in our choice by a generalization of a method introduced ten years ago by SESTERO (1964; 1966) for contact discontinuities in collisionless plasmas. Sestero considered the case in which the magnitude of B changes while the direction does not; he did not include changes in composition, temperatures, anisotropies, etc. Nevertheless, the method used here is basically the same. At each point in the transition, the velocity distribution function for each species is the sum of two different Maxwellians times step functions in the constants of motion, so that asymptotically one of these two Maxwellians becomes predominant over the other. At $X = -\infty$ and $X = +\infty$, these functions have the same first order moments ($N_1^{(\nu)}$, $T_{\perp_1}^{(\nu)}$, $T_{\parallel_1}^{(\nu)}$, V_{y_1}, V_{z_1}; $N_2^{(\nu)}$, $T_{\perp_2}^{(\nu)}$, $T_{\parallel_2}^{(\nu)}$, V_{y_2}, V_{z_2}) as the actual velocity distribution functions on each side. This choice gives the simpliest description of a transition between two distinct anisotropic displaced Maxwellian states in a multi-component plasma. However, the state of the plasma on either side of the transition does not uniquely determine the layer profile. The particular model chosen for the distribution functions determines the shape of the transition uniquely. The solution of Vlasov's equation used here corresponds to one among many other possible solutions satisfying the same asymptotic conditions. However, due to their straightforward mathematical form, these distribution functions give analytical expressions for the moments of any order.

In most cases, Poisson's equation for the electric potential can be replaced by the quasi-neutrality approximation for the charge density. The smallness of charge separation computed by evaluating the second derivative of the electric potential is a proof, *a posteriori*, of the validity of the charge neutrality assumption. Magnetic field components are obtained by numerical integration of Maxwell's equations (ROTH, 1976).

In the next section we illustrate the method for the case of a hydrogen plasma with asymptotically isotropic temperatures and no flow velocities parallel to the tangential discontinuity on either side of the magnetopause. The boundary conditions are those pertaining to the nose of the magnetosphere where the flow of the solar wind tends to vanish.

3. AN IDEAL STRUCTURE FOR THE NOSE OF THE MAGNETOPAUSE

The asymptotic values of the physical parameters representative of the Maxwellian states on both sides of the sheath are given in Table 1. These values are deduced either from observations or from the total pressure balance condition.

We assume, in the following calculations, that there is no electric potential difference ($\Delta\phi$) between $X = -\infty$ and $X = +\infty$. If the total angle of rotation of the magnetic field through the sheath is an imposed boundary condition, successive iterations are needed to fit the solution to the asymptotic conditions at $X = +\infty$ (the magnetosphere region). However, for isotropic conditions the asymptotic orientations (θ) of the magnetic field do not

Table 1. Boundary conditions pertaining to the nose of the magnetosphere

	Magnetosheath ($X = -\infty$)	Magnetosphere ($X = +\infty$)
N^- (cm^{-3})	30	1
N^+ (cm^{-3})	30	1
$T_\perp^-$ (K)	4×10^6	2×10^6
$T_\parallel^-$ (K)	4×10^6	2×10^6
$T_\perp^+$ (K)	5×10^5	3×10^5
$T_\parallel^+$ (K)	5×10^5	3×10^5
V_y (m s^{-1})	0	0
V_Z (m s^{-1})	0	0
B (nT)	5	68
θ (°)	45	87

enter into the expressions for the distribution functions, and the rate of rotation depends only on the boundary conditions and on the initial values for the vector potential components (a_y, a_z) that we choose at $X=-\infty$ (the magnetosheath region). Therefore, for the isotropic conditions used in this example, it is not necessary to impose the orientation of the magnetic field at $X=+\infty$ (the magnetosphere region) to recover the corresponding asymptotic boundary conditions. The total rotation of the magnetic field depends only (other conditions at $\pm\infty$ being unchanged) on the initial ratio $\rho(=a_y/a_z)$ on the magnetosheath side. For the case analyzed here this ratio is chosen to be 0.5.

Figure 1 shows hodograms of the magnetic field for the conditions listed in Table 1. The X-axis is in the anti-solar direction, the Y- and Z-axes are arbitrary directions in the discontinuity plane. In the magnetosheath, the magnetic field makes an angle of 45° with the Z-axis. For the particular value (0.5) of the ratio a_y/a_Z used in Fig. 1(a), the B_Z component remains constant (3.5 nT). In the magnetosphere, the angle that **B** makes with the Z-axis attains a value of 87°, indicating that the total rotation is equal to 42°. Numbers from $-\infty$ to $+\infty$ are distances along the X-axis, in units of electron skin depth, which is the classical Ferraro thickness of the magnetopause (Willis, 1971, 1975). For magnetosheath values listed in Table 1, this unit is of the order of 1 km. It can be seen that the asymptotic values of the magnetic field are rapidly attained in a few km. Figure 1(b) corresponds to a ratio $a_y/a_Z=0.995$. In this case, both the Y- and Z components of the magnetic field change. The magnetic field makes an angle of 76° with the Z-axis in the magnetosphere, the total rotation being of 31°. In the same way, by changing the value of ρ, we can obtain any angle of rotation for the magnetic field. This agrees well with experimental magnetic field measurements (Sonnerup, 1976) for which the change in direction takes any value between 0° and 180°.

The curve (ϕ) in Fig. 2 shows the electric potential profile; the potential is assumed to be zero in the magnetosheath. Across the tangential discontinuity, the electric potential rises from its minimum value of -20 V to its maximum value of 85 V in about 4 km which leads to the electric field shown in curve (E) of Fig. 2. The electric field changes sign across the transition. A maximum

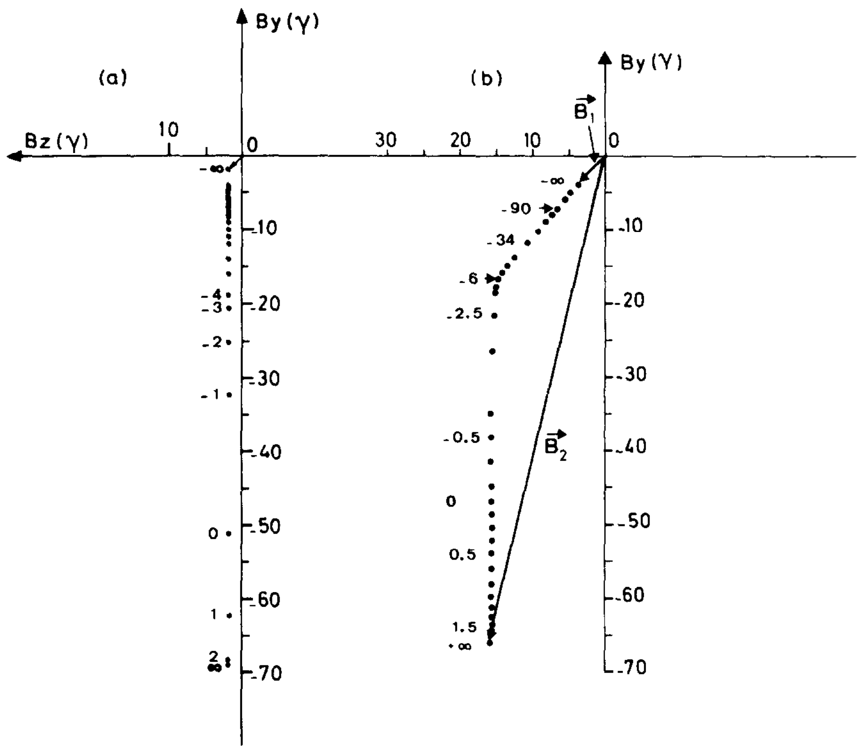

Fig. 1. Hodograms of the magnetic field (nT or γ) corresponding to the boundary conditions listed in Table 1 with $\Delta\phi=0$. (a) for $a_y/a_z=0.5$, (b) for $a_y/a_z=0.995$. Numbers from $-\infty$ to $+\infty$ are distances along the X-axis measured in electron skin depths (e.s.d.).

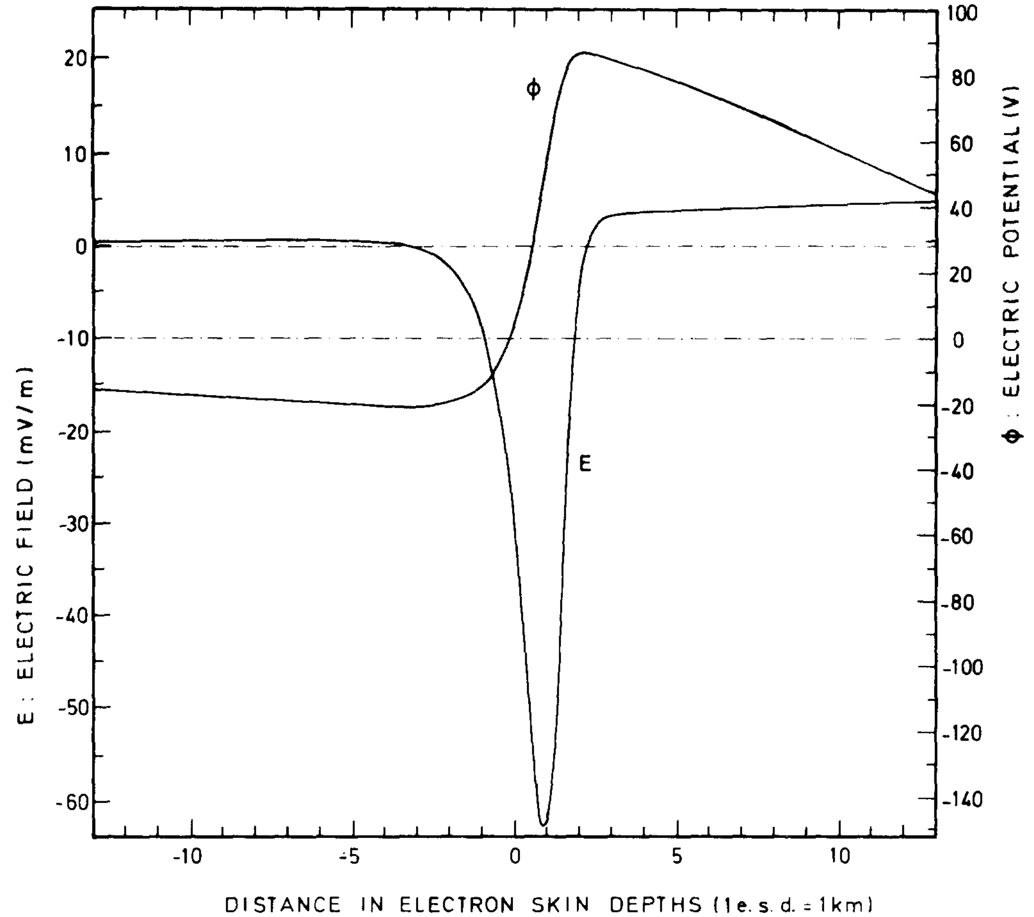

Fig. 2. Electric potential (ϕ) and electric field (E) across the sheath, corresponding to the boundary conditions listed in Table 1, with $a_y/a_z = 0.5$.

value of 67 mV/m is obtained in the centre of the sheath. This rather sharp peak of the electric field does not violate significantly the quasi-neutrality approximation. This is demonstrated in Fig. 3(a) which shows the relative charge separation $\Delta q/q$ in the centre of the sheath (Δq is the charge excess and q the charge of the electrons). The curve of Fig. 3(a) is obtained by calculating the divergence of the electric field and the corresponding charge number density according to Poisson's equation for the electric potential. The maximum relative ionic charge excess does not exceed 2×10^{-3}; this ensures *a posteriori* that the electric potential determined by the charge neutrality equation is a good approximation.

Figure 3(b) shows the number density distribution. The concentration of charged particles of either sign has a typical value of $30\,cm^{-3}$ in the magnetosheath and $1\,cm^{-3}$ in the magnetosphere. The transition occurs in a few electron skin depths. It is an example of an 'electron-dominated' layer in the sense that the electric current is mainly transported by the electrons. This is clearly illustrated in Fig. 4 where the thermal velocities ($U^{\pm}$), the drift velocities ($V_D^{\pm}$) and the Alfvén wave speed (V_A) are displayed as functions of the distance across the current layer. The top panel is for the electrons while the bottom panel is for the H^+ ions. It can be seen that most of the drift is carried by the electrons in a narrow region of thickness at most equal to a few electron skin depths. (Note the different scales in the two panels of Fig. 4.) From the curves of thermal velocities, it is seen that the temperatures do not decrease uniformly from their magnetosheath values to their magnetospheric values, but have peaks in between. This results from the particular form of the electric field in the centre of the sheath. An 'electron-dominated' layer of this

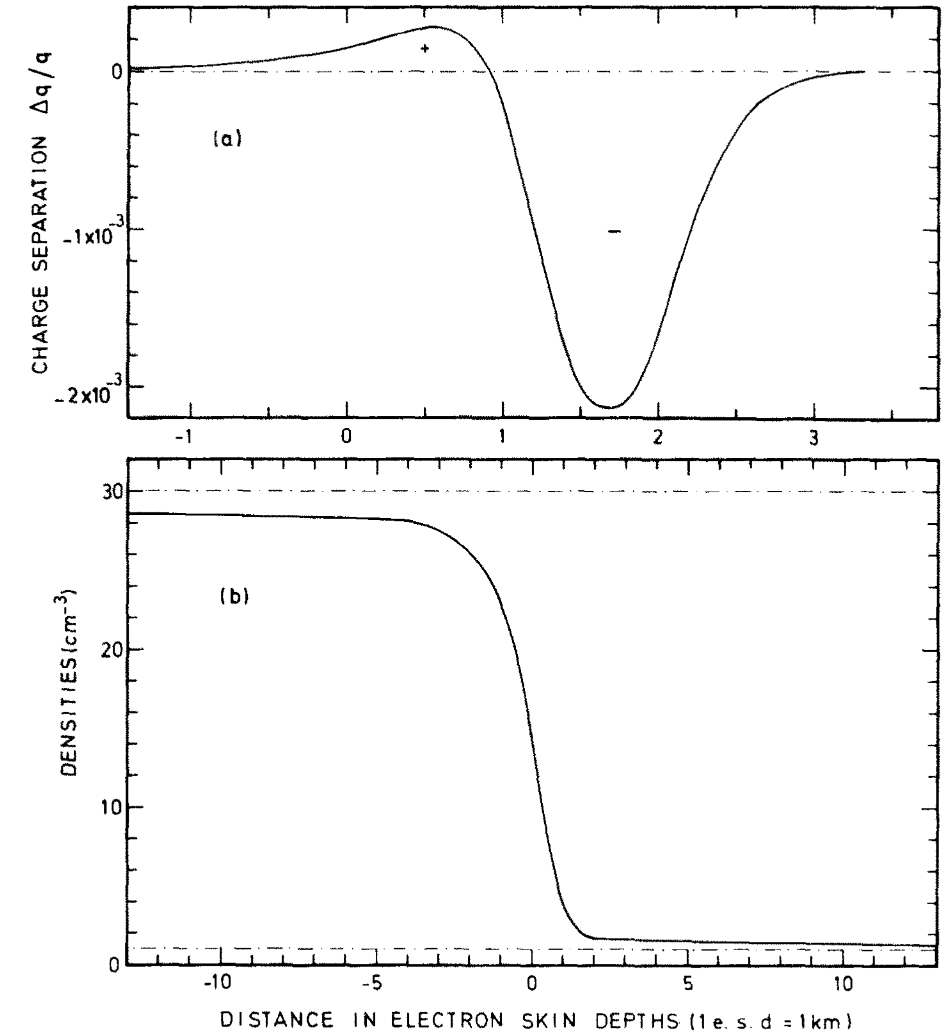

Fig. 3. (a) relative charge separation [$\Delta q/q = (\varepsilon_0/ne)\, d^2\phi/dx^2$] obtained from Poisson's equation and corresponding to the boundary conditions listed in Table 1 with $a_y/a_z = 0.5$ and $\Delta\phi = 0$. The charge separation vanishes at both sides of the sheath. (b) density of protons or electrons corresponding to the boundary conditions listed in Table 1, with $a_y/a_z = 0.5$ and $\Delta\phi = 0$.

type is certainly unstable. In the centre of the sheath, a two-stream instability will occur because the relative electron-ion mean velocity exceeds the ion thermal speed. Since the relative velocity exceeds the Alfvén wave speed in a large fraction of the unstable region, this instability is electromagnetic in character (Papadopoulos, 1973).

Other transitions with different characteristic thicknesses can be computed by changing the electric potential difference on both faces of the sheath. When this difference is such that the distribution function of one species is a Maxwellian everywhere in the transition (the temperature of this species being necessarily constant), the electric current is only due to the motion of charges carried by the other species, and the characteristic thickness is the Larmor radius of the species carrying the current. For instance, the classical Ferraro boundary layer where the ion contribution to the electric current is neglected is recovered when the ion distribution function remains a full Maxwellian. Similarly one can construct ion transitions where the electric current is only carried by the ions by assuming a full Maxwellian for the electron velocity distribution. In this case, the characteristic thickness would be of the order of 100 km, i.e. the ion gyroradius

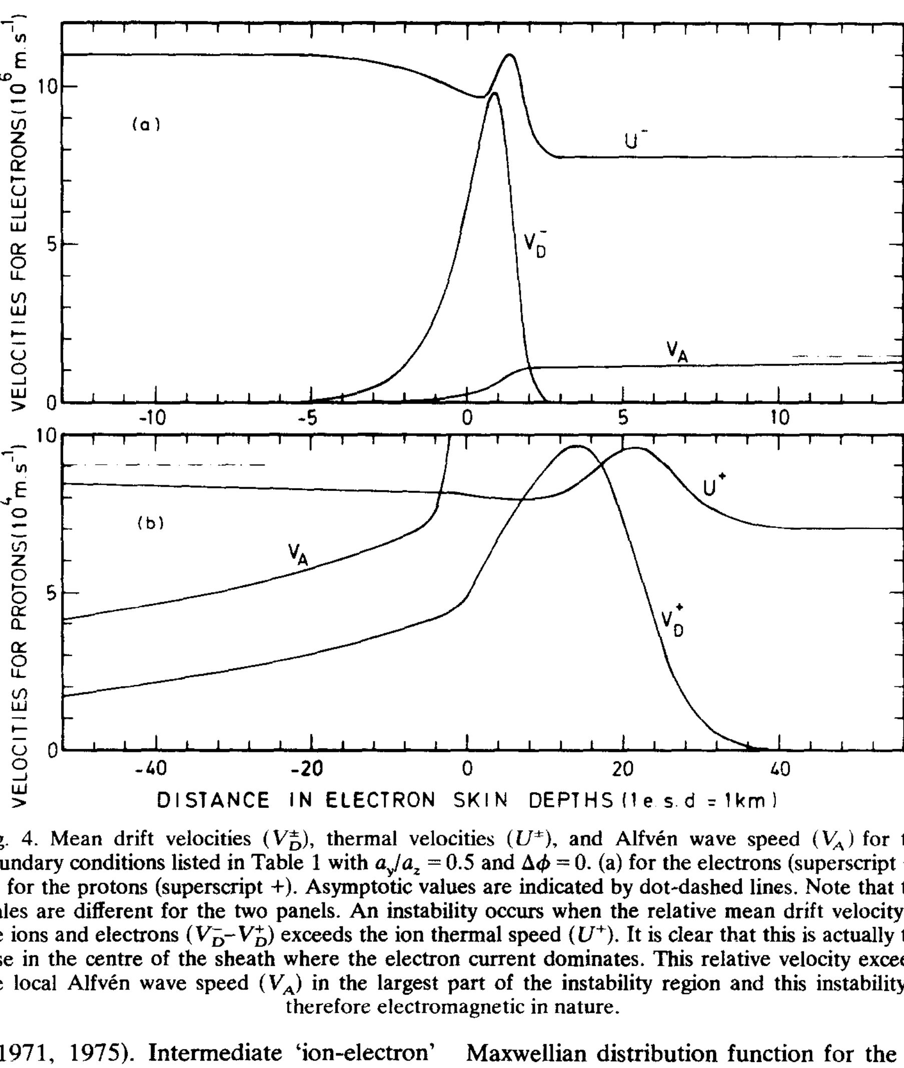

Fig. 4. Mean drift velocities ($V_D^{\pm}$), thermal velocities ($U^{\pm}$), and Alfvén wave speed (V_A) for the boundary conditions listed in Table 1 with $a_y/a_z = 0.5$ and $\Delta\phi = 0$. (a) for the electrons (superscript −). (b) for the protons (superscript +). Asymptotic values are indicated by dot-dashed lines. Note that the scales are different for the two panels. An instability occurs when the relative mean drift velocity of the ions and electrons ($V_D^- - V_D^+$) exceeds the ion thermal speed (U^+). It is clear that this is actually the case in the centre of the sheath where the electron current dominates. This relative velocity exceeds the local Alfvén wave speed (V_A) in the largest part of the instability region and this instability is therefore electromagnetic in nature.

(Willis, 1971, 1975). Intermediate 'ion-electron' layers are found when we vary the electric potential difference between its characteristic values for 'true' electron and ion layers and/or when we introduce temperature differences between the two sides of the sheath.

4. CONCLUSIONS

In this paper, we have described a possible structure for the magnetopause near the nose region. With no electric potential difference between the two sides of the sheath, the results of the computations show an 'electron-dominated' layer in the sense that the electric current is carried mainly by the electrons. However, this boundary layer is found unstable. This instability will force the electrons to become more isotropic and this will finally broaden the layer. Ideally, such a broadened current layer can be obtained by assuming a full Maxwellian distribution function for the electrons. In such a case, the ions alone contribute to the current. Since an 'electron-dominated' layer of the kind described here is unstable, it is not necessary, in order to broaden the layer, to discharge the polarization electric field by means of ionospheric charges coming up along the high latitude field lines (Parker, 1967); a two-stream instability can be adequate for this broadening. We can construct 'true' ion (or electron) layers by imposing a suitable electric potential difference between the two faces of the sheath, in order to keep the electron (or ion) velocity distribution Maxwellian everywhere. In this way, the electric potential is seen to control the thickness of the layer.

Acknowledgements—The author would like to thank Prof. M. Nicolet for his continual interest during the preparation of this paper, and Dr. J. Lemaire for discussions and comments.

REFERENCES

ALPERS W. 1969 *Astrophys. Space Sci.* **5**, 425.
ALPERS W. 1971 *Astrophys. Space Sci.* **11**, 471.
CUMMINGS W. D. and COLEMAN P. J. 1968 *J. geophys. Res.* **73**, 5699.
FERRARO V. C. A. 1952 *J. geophys. Res.* **57**, 15.
KAN J. R. 1972 *J. Plasma Phys.* **7**, 445.
LEMAIRE J. and BURLAGA L. F. 1976 *Astrophys. Space Sci.* **45**, 303.
NEUGEBAUER M., RUSSELL C. T. and SMITH E. J. 1974 *J. geophys. Res.* **79**, 499.
PAPADOPOULOS K. 1973 *Astrophys. J.* **179**, 939.
PARKER E. N. 1967 *J. geophys. Res.* **72**, 4365.
SESTERO A. 1964 *Physics Fluids* **7**, 44.
SESTERO A. 1966 *Physics Fluids* **9**, 2006.
SONNERUP B. U. O. 1976 *Physics of Solar Planetary Environments*, (Edited by D. J. WILLIAMS) *Proceedings of International Symposium on Solar-Terrestrial Physics*, Boulder, Co., June 1976 *Am. Geophys. U.*, p. 541.
SONNERUP B. U. O. and LEDLEY B. G. 1974 *J. geophys. Res.* **79**, 4309.
WILLIS D. M. 1971 *Rev. Geophys. Space Phys.* **9**, 953.
WILLIS D. M. 1975 *Geophys. J. R. Astron. Soc.* **41**, 355.

Reference is also made to the following unpublished material:

ROTH M. 1976 Structure of a tangential discontinuity in a multi-component Vlasov plasma (to be submitted as part of Ph.D. thesis).